ELSEVIER

Desalination 150 (2002) 65–74

DESALINATION

www.elsevier.com/locate/desal

Effect of asymmetry in a bipolar membrane on water dissociation — a mathematical analysis

Tongwen Xu

Department of Chemistry, University of Science and Technology of China, Hefei 230026, China
Tel. +86 (551) 360-1587; email: twxu@ustc.edu.cn

Received 28 August 2001; accepted 24 March 2002

Abstract

Based on a simple model established in the previous paper for water dissociation process on a bipolar membrane, this work is concentrated on analyzing the membrane asymmetry on the water dissociation process. Special attention is paid to thickness ratio, fixed group concentration ratio and the water diffusivity ratio of anion layer to cation layer on water concentration, proton or hydroxyl ions concentration in the depletion layer as well as the current density curves. The results suggest that for practical applications, an asymmetric bipolar membrane with the appropriate thickness, proper ion-exchange capacity and high permeability to water will receive more effective results than a symmetric one.

Keywords: Bipolar membrane; Water dissociation; Current voltage characteristics; Asymmetry

1. Introduction

A bipolar membrane (BM) is composed of a cation (with negatively fixed charge) and an anion ion-exchange layer (with positively fixed charge) joined together in series. Just the same as the discovery of N-P junctions in semiconductor technology, this composition brings about many novelties to a bipolar membrane, making it useful in many new technological applications [1–4], most of which originate from its ability to dissociate water when high reverse voltage is applied. Its potential as a water-splitting technology has attracted many investigations. But the actual mechanism causing this splitting remains a matter of controversy, and at present no model can completely explain all the phenomena existing in a water dissociation process [5,6]. Up to now, three physical models have been proposed: Second Wien Effect Model (SWEM) [7], Chemical Reaction Model (CRM) [8] and Neutral Layer Model (NLM) [9], providing a theoretical basis to investigate this water dissociation process. Theories based on these models have explained some particular experimental phenomena to some extent. However, among them, SWEM seems to be most widely

0011-9164/02/$– See front matter
PII: S0011-9164(02)00930-X

accepted [10,11]. This model assumed that there is a dry "space charge region" [12] or "depletion layer" [13] at the transition layer (TRL), i.e., the junction between the cation and anion layers where the mobile ions have much smaller concentrations than the fixed charge [10–14]. When high reverse voltage is applied, just as the same as that in a double-layer biological membrane containing fixed charge and exhibiting rectification and capacitance properties, water dissociation occurs mainly at this zone and behaves as a weak electrolyte. Theories based on these assumptions allowed for reasonable explanation of experimental facts [10,11,14–19]. The existence of a depletion layer at the junction is also supported by the recent investigations in terms of the measurements of AC conductance at low frequency [20]. But the existing models for water dissociation were derived from the viewpoint of an identical structure of the anion and cation layers composed of a bipolar membrane [3,4,8–12,14–19].

The main purpose of this job is to simulate the asymmetry of the cation and anion layers on the water dissociation curve, proton or hydroxyl ion and water concentration in the depletion layer based on a simple model which was previously established to describe the voltage current characteristics base on both SWEM [7] and Space Charge Theory [12] from the viewpoint of chemical engineering (equation of continuity) and unsteady state [21].

2. Model and basic equations

A bipolar membrane considered here consists of an anion and a cation selective layer joined together with a TRL at the junction when an electric field is established across the membrane. The thickness of anionic and cationic exchange layers is d_m^A and d_m^C, the fixed charge concentration of the two layers is X_m^A and X_m^C, and the diffusion coefficient of water through the layers is $D_{H_2O}^A$ and $D_{H_2O}^C$, respectively. The transition layer is depleted of ions and has a total thickness of $\lambda=\lambda_N+\lambda_P$, where λ_N and λ_P correspond to the depletion thickness in the negatively and positively charged layers. As described in a previous paper [21], the model is derived based on the following assumptions which were shown to be reasonable [6,7,10,11,16–19].

1. Water dissociation mainly occurs in the transition or depletion layer and the dissociated ions removed from this region are replenished by the following water dissociation equilibrium:

$$H_2O \underset{k_{-1}}{\overset{k_1}{\longleftrightarrow}} H^+ + OH^-$$

2. The water dissociation is accelerated by the electric field according to the second Wien effect which describes the influence of a strong electric field E on the water dissociation constant k_1 while the recombination rate constant k_{-1} is not affected by the electric field.

$$\frac{k_1}{k_1^0} = \left(\frac{2}{\pi}\right)^{1/2} (8b)^{-3/4} \exp\left[(8b)^{1/2}\right] \qquad (1)$$

with $b = 0.09636 \dfrac{E}{\varepsilon_r T^2}$, where ε_r is the relative permittivity, k_1 is the forward rate constant of the net reaction responsible for the electric field enhanced water dissociation and k_1^0 is the forward rate constant of the reaction when no external electric field is applied.

3. The generated protons and hydroxyl ions are removed from the transition region by migration and the consumed water can be compensated timely by diffusion from the bulk solution.

4. The electric current is calculated from the migration flux of either protons or hydroxyl ions.

5. The voltage drops across both anion and

cation exchange layers are neglected so that voltage across a bipolar membrane is equal to that across the transition region U^{tr} and the driving force for the migration of ions is U^{tr}/λ, since the Donnan potential is in equilibrium with the diffusion of ions into the transition region.

6. Based on the Poisson equation, the electric field density E and the total depletion thickness can be related to the potential drop applied in the depletion layer, U^{tr}, as follows [10,12,17,19]:

$$E = \left[\frac{2F}{\varepsilon_r \varepsilon_0} U^{tr} \frac{X_m^A X_m^C}{X_m^A + X_m^C}\right]^{1/2} \tag{2}$$

$$\lambda = \lambda_N + \lambda_P = \left[\frac{2\varepsilon_r \varepsilon_0}{F} U^{tr} \frac{X_m^A + X_m^C}{X_m^A X_m^C}\right]^{1/2} \tag{3}$$

where ε_0 is the permittivity of free space, F is the Faraday constant, and U^{tr} is the voltage across the transition region.

Using the equation of continuity and transport theory, the concentration change of different species in the transition layer was obtained as [21])

$$\frac{dc_{H^+}^{tr}}{dt} = k_1 c_{H_2O}^{tr} - k_{-1} c_{H^+}^{tr} c_{OH^-}^{tr} - \frac{u_{H^+}^{tr} c_{H^+}^{tr}}{\lambda} \frac{U^{tr}}{\lambda} \tag{4}$$

$$\frac{dc_{OH^-}^{tr}}{dt} = k_1 c_{H_2O}^{tr} - k_{-1} c_{H^+}^{tr} c_{OH^-}^{tr} - \frac{u_{OH^-}^{tr} c_{OH^-}^{tr}}{\lambda} \frac{U^{tr}}{\lambda} \tag{5}$$

$$\frac{dc_{H_2O}^{tr}}{dt} = k_{-1} c_{H^+}^{tr} c_{OH^-}^{tr} - k_1 c_{H_2O}^{tr} + \frac{D_{H_2O}^A}{\lambda} \frac{c_{H_2O}^A - c_{H_2O}^{tr}}{d_m^A} + \frac{D_{H_2O}^C}{\lambda} \frac{c_{H_2O}^C - c_{H_2O}^{tr}}{d_m^C} \tag{6}$$

where $u_{H^+}^{tr}$, $u_{OH^-}^{tr}$, $c_{H^+}^{tr}$ and $c_{OH^-}^{tr}$ are the respective mobilities and concentrations of protons and hydroxyl ions in the transition layer and $c_{H_2O}^{tr}$ is the concentration of water in the transition layer. Therefore, the electric current density can be calculated from the hydroxyl ion or proton flux as follows based on assumption (2):

$$I = F u_{OH^-}^{tr} c_{OH^-}^{tr} \frac{U^{tr}}{\lambda} = F u_{H^+}^{tr} c_{H^+}^{tr} \frac{U^{tr}}{\lambda} \tag{7}$$

Eqs. (4)–(7) allow a theoretical simulation of proton, hydroxyl ion and water concentration in the depletion layer as well as I-V curves by assuming the asymmetrical structure of bipolar membranes.

3. Results and discussion

To determine the steady state of the described system, the three differential Eqs. (4)–(6) were solved as a function of time by using the parameters listed in Table 1.

Fig. 1 shows the proton and hydroxyl ion concentration in the transition region as a function of time. Though the concentrations of both H^+ and OH^- change with the time, the electroneutrality is preserved due to the assumed equal mobility of H^+ and OH^-. At 10^{-4} s, the steady state is reached with $C_H^{tr} = C_{OH}^{tr} = 4.49 * 10^{-4}$ mol.m^{-3}

The calculated current density is shown in Fig. 2, which behaves analogous to that of the

Table 1
Typical parameters used for calculations

Parameter	Value	Source
Faraday constant, F	96,486 A.s.mol^{-1}	
Permittivity of free space, ε_0	8.85*10^{-12} A.s.V^{-1} m^{-1}	Universal
Dissociation rate constant, k_1^0	2×10^{-5} s^{-1}	Constants
Combination rate constant, k_{-1}	1.1×10^{8} m^3.mol^{-1} .s^{-1}	
Mobility of protons in TRL, u_H^{tr}	30.0×10^{-8} m^2.V^{-1}.s^{-1}	
Mobility of hydroxyl ion in TRL, u_{OH}^{tr}	30.0×10^{-8} m^2.V^{-1}.s^{-1}	Adapted from
Relative permittivity in TRL, ε_r	20	[6,22,23]
Initial conc. of proton and hydroxyl in TRL, $C_H^{tr,0}$, $C_{OH}^{tr,0}$	10^{-4} mol.m^{-3} (10^{-7} mol.L^{-1})	
Conc. of water in BM, $C_{H_2O}^{bm}$	6000 mol.m^{-3}	
Initial conc. of water in TRL, $C_{H_2O}^{tr,0}$	6000 mol.m^{-3}	
Temperature, T	293.15 K	
Thickness of the layers, d	10^{-4} m	Experimental
Diffusion coefficient of water in both layers, D_{H_2O}	10^{-9} m^2.s^{-1}	determination
Conc. of fixed groups, X	1.5×10^{3} mol.m^3	

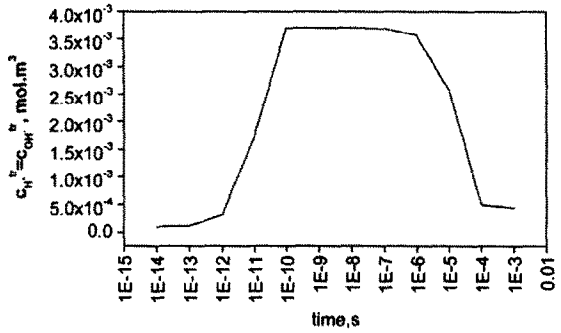

Fig. 1. Concentration of H^+ and OH^- as a function of time.

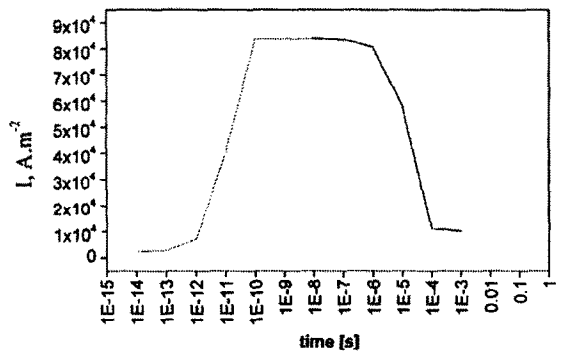

Fig. 2. Current density as a function of time.

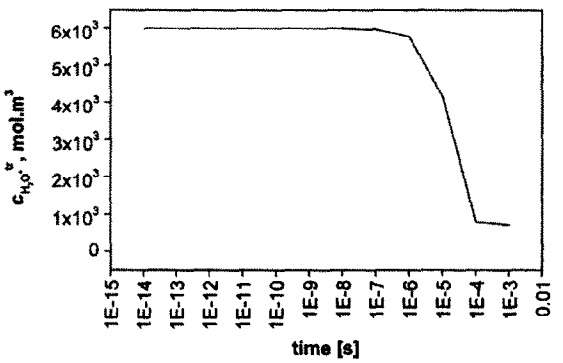

Fig. 3. Water concentration in the transition region as a function of time.

proton and hydroxyl ion concentration in the transition region. Fig. 3 illustrates the decreasing water concentration in the transition region due to the consumption of water by the water dissociation. It is also shown that the steady state is reached at 10^{-4} s with $C_{H_2O}^{tr} = 726$ mol.m^3. For a conventional water dissociation process, this short time is fully assured, thus the following simulation is based on the steady state.

3.1. Effect of the thickness ratio

Figs. 4–6 demonstrate the effect of the thickness ratio of the cation layer to the anion layer. Two situations had to be considered. One is the case that either the cation or anion layer is fixed and the other is that total thickness of a bipolar membrane is fixed. If the cation layer is fixed, it was observed that an increase in the thickness ratio gives rise to a decrease in the concentrations of proton and water in the transition zone as well as a current density decrease at the given applied voltage. An increase in the thickness ratio will also result in the changes of the current voltage profiles, which show that the limiting current density is decreased, especially for the case where the ratio is smaller than 0.5. For example, when the ratio changes from 0.1 to 1, the limiting current density decreased from 640,000 to 115,000 $A.m^{-2}$; when the ratio changes from 1 to 10, the limiting current density decreased from 115,000 to 6170 $A.m^{-2}$. This is because an increase in layer thickness ratio will correspondingly cause an increase in total membrane thickness, giving rise to an increase in diffusion resistance of a bipolar membrane. In addition, an increase in layer thickness will increase the diffusional resistance of water and water ions from the outer bulk solution, so the limiting current density is decreased. If the thickness of a bipolar membrane remains unchanged, i.e., $d_m^A + d_m^C$ = constant, the shape of the profiles for water and water ions in the transition layer as well as I-V is the same as the above, but the relative magnitude is changed. As shown in Figs. 7–9, the less or the larger the thickness ratio is, the larger the water and water ions concentration as well as the current density are. The minimum for these parameters appear at the case of thickness ratio=1. It suggests that, a bipolar membrane with an asymmetrical thickness of cation and anion layer will have a better performance.

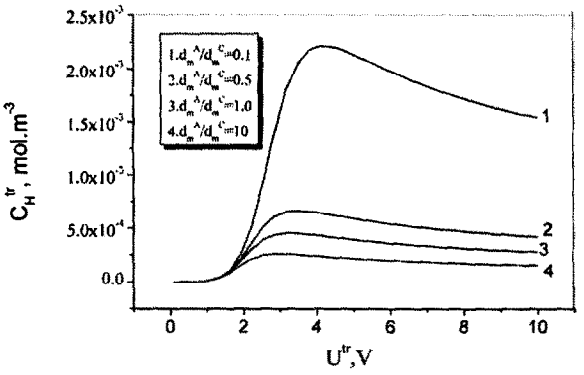

Fig. 4. Influence of thickness ratio on C_H^{tr}, $d_m^C = 10^{-4}$m.

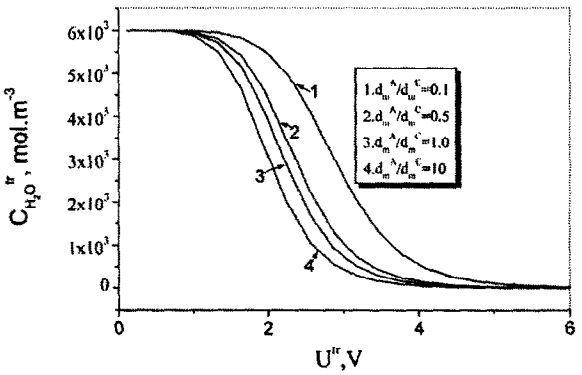

Fig. 5. Influence of thickness ratio on $C_{H_2O}^{tr}$, $d_m^C = 10^{-4}$m.

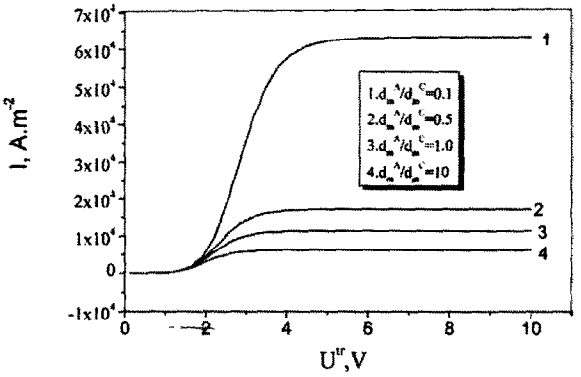

Fig. 6. Influence of thickness ratio on the current voltage curve, $d_m^C = 10^{-4}$m.

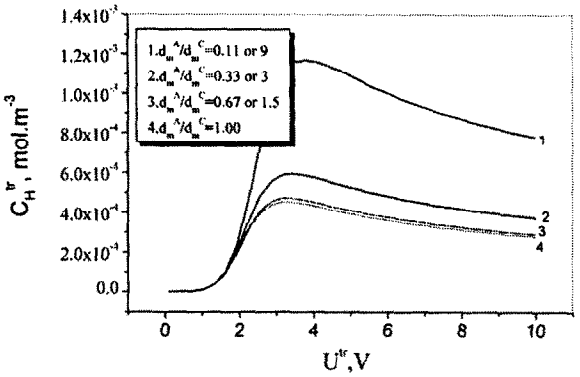

Fig. 7. Influence of thickness ratio on $C_H^{tr}\ d_m^A + d_m^C = 2e^{-4}$m.

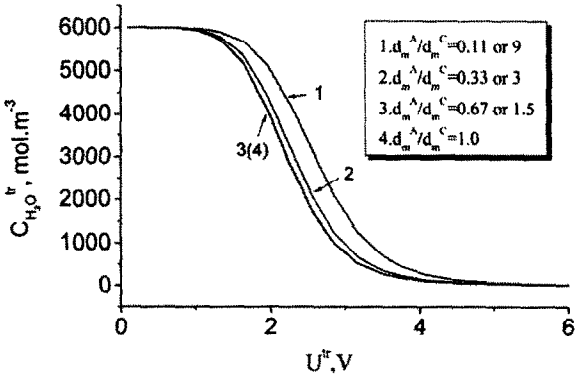

Fig. 8. Influence of thickness ratio on $C_{H_2O}^{tr}\ d_m^A + d_m^C = 2e^{-4}$ m.

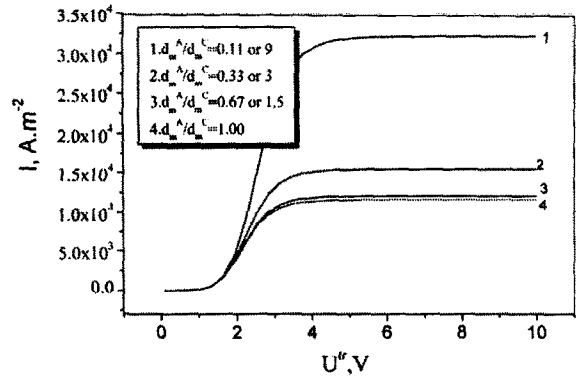

Fig. 9. Influence of thickness ratio on the current voltage curve $d_m^A + d_m^C = 2e^{-4}$ m.

3.2. Effect of water diffusivity ratio

The effects of water diffusivity ratio on the dissociation rate are illustrated in Figs. 10–12 for the case where water diffusivity is constant in the cation layer. It was demonstrated that water and water ions concentrations in the TRL, limiting current density, decrease when the water diffusivity ratio decreases. A theoretical interpretation of this is that when the water diffusivity ratio decreases, water flux into the TRL decreases and the water, which has been dissociated into protons and hydroxyl ions, cannot be compensated by the water transported into the membrane due to diffusion, which thus causes a decrease in water concentration therein. Correspondingly, the concentrations of protons and hydroxyl ions depend on the water concentration and will decrease with a decrease in water concentration in TRL as shown in Fig. 11. Thus, the observable current density as calculated from Eq. (14) is also decreasing as shown in Fig. 12. It should be noted that if the water concentration in the TRL reaches a very small value, the water dissociation and hence the current density will be limited by the diffusion of water into the membrane. Therefore, in practical operations, a bipolar membrane with high water diffusivity is strongly recommended for enhancing water splitting and saving energy.

It should be noted that both water and water ions concentration as well as I-V characteristics are only affected by the total water diffusivity in cation and anion layers. Therefore, if $D_{H_2O}^A + D_{H_2O}^C$ = constant, current density, water and water ions concentrations will be independent of the water diffusivity ratio. This result can be clearly observed from model Eqs. (4)–(6).

3.3. Effect of fixed group concentration ratio

Figs. 13–15 show the effects of fixed group concentration ratio on water and water ions

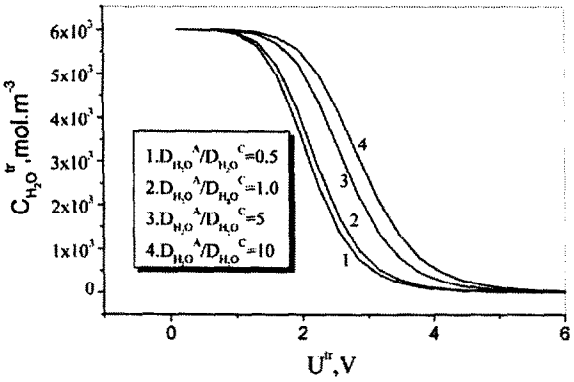

Fig. 10. Influence of $D^{A}_{H_2O}/D^{C}_{H_2O}$ on $C^{tr}_{H_2O}$ $D^{C}_{H_2O} = 1e^{-9}$.

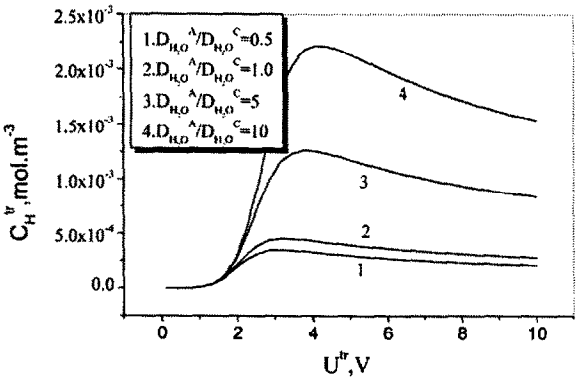

Fig. 11. Influence of $D^{A}_{H_2O}/D^{C}_{H_2O}$ on C^{tr}_{H} $D^{C}_{H_2O} = 1e^{-9}$.

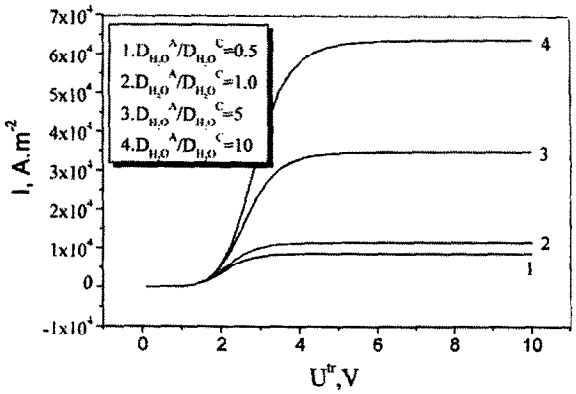

Fig. 12. Influence of $D^{A}_{H_2O}/D^{C}_{H_2O}$ on the current voltage curve $D^{C}_{H_2O} = 1e^{-9}$.

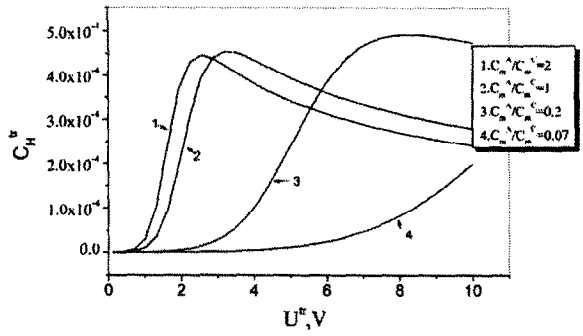

Fig. 13. Influence of C^{A}_{m}/C^{C}_{m} on C^{tr}_{H}, $C^{C}_{m} = 1500$.

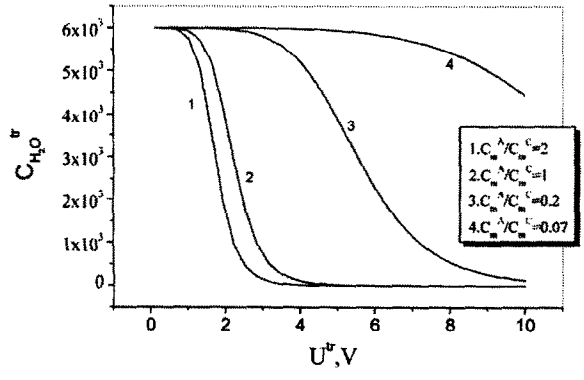

Fig. 14. Influence of C^{A}_{m}/C^{C}_{m} on $C^{tr}_{H_2O}$, $C^{C}_{m} = 1500$.

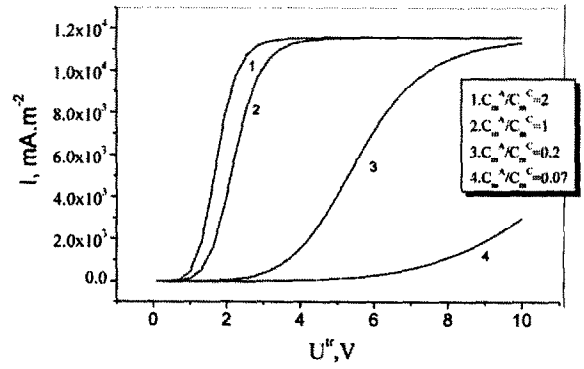

Fig. 15. Influence of C^{A}_{m}/C^{C}_{m} on the current voltage curve $C^{C}_{m} = 1500$.

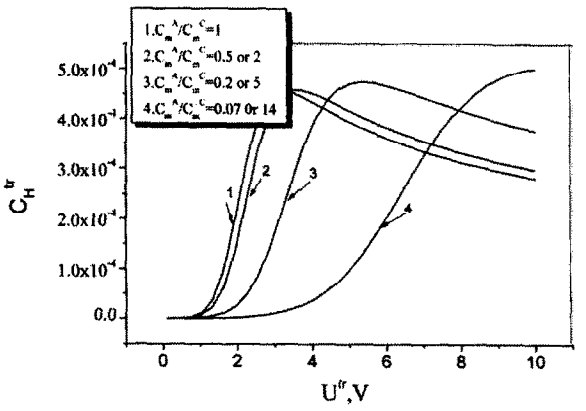

Fig. 16. Influence of C_m^A/C_m^C on $C_H^{tr}C_m^A+C_m^C=3000$.

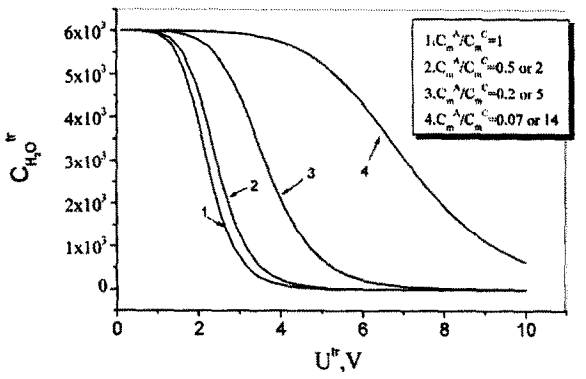

Fig. 17. Influence of C_m^A/C_m^C on $C_{H_2O}^{tr}C_m^A+C_m^C=3000$

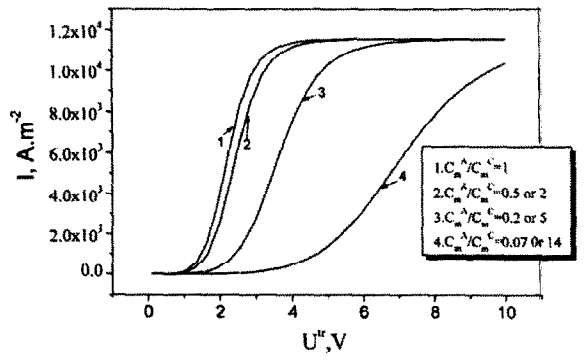

Fig. 18. Influence of C_m^A/C_m^C on the current voltage curve $C_m^A+C_m^C=3000$.

concentration as well as I-V curves when C_m^C is constant. Unlike the thickness ratio, a change in a fixed group concentration ratio will cause changes not only in relative magnitude but also in the shape of the profiles. Take proton concentration as an example: the curves seem to be more complicated than the above. There is a maximum in each profile; an increase in the fixed group concentration ratio will cause a decrease in proton concentration before the maximum. But after the maximum, the trends are reversed. The larger the fixed group concentration ratio, the smaller the voltage drop corresponding to the maximum concentration. The profiles for water concentration and current voltage can be analyzed in the same way. The effect of the fixed group concentration ratio on water dissociation can be observed from the I-V curves. As shown in Fig. 15, with the increasing fixed group concentration ratio, water dissociation speeds up and thus the water concentration in the transition zone is decreased due to the increasing consumption of water as shown in Fig. 14. The limiting current density seems to be independent of the fixed group concentration ratio, but the voltage attaining the limiting current density is smaller when the fixed group concentration ratio is larger. This suggests that low energy is needed to dissociate water at a high fixed group concentration ratio.

If $C_m^A+C_m^C$ remain constant, the shape of the profiles for water and water ions in the transition layer as well as I-V stay approximately unchanged as shown in Figs. 16–18. The above analyses are still applicable, but it should be noted that in this case the maximum water and water ions concentration as well as current density appear in the case of $C_m^A=C_m^C$.

4. Conclusions

Based on a simple model established in the previous paper for the theoretical current voltage

characteristics in water dissociation process on a bipolar membrane, the effect of asymmetry of the cation and anion layers in a bipolar membrane was mathematically simulated for the water dissociation process. Particular attention was given to the influence of the thickness ratio, fixed group concentration ratio and water diffusivity ratio of the anion layer to cation layer on water and water ions concentrations in the TRL and current voltage curve.

Evaluated by the I-V curves, the better performance of a bipolar membrane is not the one with the identical cation and anion structures. If the total parameters of a bipolar membrane are fixed, such as $d_m^A + d_m^C$, $C_m^A + C_m^C$ and $D_{H_2O}^A + D_{H_2O}^C$ remain constant, the lowest voltage appears for the case of the thickness ratio = minimum, fixed group concentration ratio = 1 and is independent of the water diffusivity ratio. If the parameters of one layer are fixed, such as d_m^C, C_m^C, $D_{H_2O}^C$ are fixed, the lowest voltage appears at the case of thickness ratio = minimum, fixed group concentration ratio = maximum and water diffusivity ratio = maximum. Therefore, for practical applications, an asymmetric bipolar membrane in thickness with a proper ion-exchange capacity and high permeability to water will obtain more effective results than a symmetric one.

5. Symbols

c — Concentration for water and water ions, mol.m^{-3}
d — Thickness, m
E — Electrical field strength, V.m^{-1}
F — Faraday constant, 96,486 A.s.mol^{-1}
I — Current density, A.M^{-2}
R — Gas constant, 8.314 J.mol^{-1}.K^{-1}
T — Temperature, K
t — Time, s
U — Potential drop, V
u — Mobility, cm^2 s^{-1}.V^{-1}
X — Fixed group concentration of monolayer, mol.m^{-3}

Greek

ε_0 — Permittivity of free space, 8.85* 10^{-12}, A.s.V^{-1}.m^{-1}
ε_r — Relative permittivity
λ — Thickness in transition layer

Superscripts

A — Anion exchange layer
bm — Bipolar membrane
C — Cation exchange layer
tr — Transition layer
0 — Initial value ($t = 0$)

Subscripts

m — Membrane phase
H^+ — Protons
OH^- — Hydroxyl ions
H_2O — Water

Acknowledgements

Financial support from the Natural Science Foundation of China (No. 29976040,20106015), the Key Foundation of the Educational Committee of Anhui Province (2000jl255zd), the Natural Science Foundation of Anhui Province (99045431), and the Foundation of Resources and the Environment of the University of Science and Technology of China are gratefully acknowledged. The author would also like to express his special thanks to Mr. G.C. Yan for writing the computing programs.

References

[1] T.W. Xu, Development of a bipolar membrane-based process. Desalination, 140 (2001) 247–258.

[2] T. Tsuru, S. Nakao and S. Kimura, Ion separation by bipolar membranes in reverse osmosis, J. Membr. Sci., 108 (1995) 269–278.
[3] B. Bauer, F.J. Gerner and H. Strathmann, Development of bipolar membranes, Desalination, 68 (1988) 279–292.
[4] K.N. Mani, Electrodialysis water splitting technology, J. Membr. Sci., 58 (1991) 117–138.
[5] R. Simons, Electric field effects on proton transfer between ionizable groups and water in ion exchange membranes, Electrochim. Acta, 29 (1984) 151–158.
[6] H. Strathmann., J.J. Krol, H.J. Rapp [all authors??], Limiting current density and water dissociation in bipolar membranes, J. Membr. Sci., 125 (1997) 123–142.
[7] L. Onsager, Deviations from Ohm's Law in weak electrolytes, J Chem. Phys., 2 (1934) 599–612.
[8] R. Simons, Strong electric fields effects on proton transfer between membrane-bound amines and water, Nature, 280 (1979) 824–826.
[9] R. Simons and G. Khanarian, Water dissociation in bipolar membranes: experiments and theory, J. Membr. Biol., 38 (1978) 11–30.
[10] H. Holdik, A. Alcaraz, P. Ramirez, [all authors??], Electric field enhanced water dissociation at the bipolar junction from ac impedance spectra measurements, J. Electroanatical Chem., 442 (1998) 13–18.
[11] S. Mafe, P. Ramirez and A. Alcaraz, Electric field-assisted proton transfer and water dissociation at the junction of a fixed-charged bipolar membrane, Chem. Phys. Lett., 294 (1998) 406–412.
[12] A. Mauro, Space charge region in fixed charge membranes and the associated property of capacitance, Biophysical J., 2 (1962) 179–197.
[13] R, Simons, The steady and non steady state properties of bipolar membranes, Biochim. Biophys. Acta, 274 (1972) 1–14.
[14] H.G.L. Coster, The double fixed charge membrane, Biophysical J., 13 (1973) 118–132.
[15] T.C. Chilcott, H.G.L. Coster and E.P. George, AC impedance of the bipolar membrane at low and high frequencies, J. Membr. Sci., 100 (1995) 77–86.
[16] H.G.L. Coster, A quantitative analysis of the voltage-current relationships of fixed charge membranes and the associated property of 'punch-through', Biophysical J.,5 (1965) 669–679.
[17] S. Mafe and J.A. Manzanares, Model for ion transport in bipolar membranes, Phys. Rev. A, 42 (1990) 6245–6248.
[18] P. Ramirez, J.A. Manzanares and S. Mafe, Water dissociation effects in ion transport through anionic exchange membranes with thin cationic exchange surface films, Ber. Bunsenges Phys. Chem., 95(1) (1991) 499–503.
[19] R.A. Simons, Mechanism for water flow in bipolar membranes, J. Membr. Sci., 82 (1993) 65–73.
[20] J.R. Smith, R. Simons and J. Weidenhaun, The low frequency conductance of bipolar membranes demonstrates the presence of a depletion layer, J. Membr. Sci., 140 (1998) 155–164.
[21] T.W. Xu, W.H. Yang and B.L. He, A simple model to determine the trends of electric field enhanced water dissociation in a bipolar membrane, Chi. J. Chem. Eng., 9(2) (2001) 179–185.
[22] T.W. Xu W.H. Yang and B.L. He, Water dissociation phenomena in a bipolar membrane — the configurations and theoretical voltage analysis, Sci. China, 42(6) (1999) 589–598.
[23] P.W. Atkins, Physical Chemistry, 5th ed., Oxford University Press, Oxford, UK, 1994.